HYDROGEN JET FIRES IN A PASSIVELY VENTILATED ENCLOSURE

Hooker, P.[1], Hall, J.[2], Hoyes, J.R.[3], Newton, A.[4] and Willoughby, D.[5]
[1] Major Hazards Unit, HSL, Harpur Hill, Buxton, SK17 9JN, U.K., philip.hooker@hsl.gsi.gov.uk
[2] Major Hazards Unit, HSL, Harpur Hill, Buxton, SK17 9JN, U.K., jonathan.hall@hsl.gsi.gov.uk
[3] Mathematical Sciences Unit, HSL, Harpur Hill, Buxton, SK17 9JN, U.K.,
james.hoyes@hsl.gsi.gov.uk
[4] Mathematical Sciences Unit, HSL, Harpur Hill, Buxton, SK17 9JN, U.K.,
andrew.newton@hsl.gsi.gov.uk
[5] Major Hazards Unit, HSL, Harpur Hill, Buxton, SK17 9JN, U.K.,
deborah.willoughby@hsl.gsi.gov.uk

ABSTRACT

This paper describes a combined experimental, analytical and numerical modelling investigation into hydrogen jet fires in a passively ventilated enclosure. The work was funded by the EU Fuel Cells and Hydrogen Joint Undertaking project Hyindoor. It is relevant to situations where hydrogen is stored or used indoors. In such situations passive ventilation can be used to prevent the formation of a flammable atmosphere following a release of hydrogen. Whilst a significant amount of work has been reported on unignited releases in passively ventilated enclosures and on outdoor hydrogen jet fires, very little is known about the behaviour of hydrogen jet fires in passively ventilated enclosures. This paper considers the effects of passive ventilation openings on the behaviour of hydrogen jet fires. A series of hydrogen jet fire experiments were carried out using a 31 m^3 passively ventilated enclosure. The test programme included subsonic and chocked flow releases with varying hydrogen release rates and vent configurations. In most of the tests the hydrogen release rate was sufficiently low and the vent area sufficiently large to lead to a well-ventilated jet fire. In a limited number of tests the vent area was reduced, allowing under-ventilated conditions to be investigated. The behaviour of a jet fire in a passively ventilated enclosure depends on the hydrogen release rate, the vent area and the thermal properties of the enclosure. An analytical model was used to quantify the relative importance of the hydrogen release rate and vent area, whilst the influence of the thermal properties of the enclosure were investigated using a CFD model. Overall, the results indicate that passive ventilation openings that are sufficiently large to safely ventilate an unignited release will tend to be large enough to prevent a jet fire from becoming under-ventilated.

1.0 NOMENCLATURE

g'_e reduced gravity of gas in enclosure (m s^{-2})
g acceleration due to gravity (m s^{-2})
B_0 buoyancy flux (m^4 s^{-3})
     vent exchange flow coefficient (dimensionless)
A area of the vent (m^2)
d height of the vent (m)
C entrainment constant (dimensionless)
h height of interface between buoyant and ambient fluids (m)
Q_c convective power of the fire (J s^{-1})
T_a ambient temperature (K)
$_a$ ambient density (kg m^{-3})
c_{pa} specific heat capacity (J K^{-1} mol^{-1})
T_e temperature within enclosure (K)
P_a ambient pressure (Pa)
R universal gas constant (8.314 J K^{-1} mol^{-1})
M_e molecular weight of gas in enclosure (g mol^{-1})

2.0 INTRODUCTION

Hydrogen energy applications may require that systems be used inside rooms or enclosures (e.g. for security or safety reasons). The ignition of accidentally released hydrogen may result in a jet-fire. This paper describes experiments, analytical modelling and CFD modelling that has been carried out by the United

Kingdom's Health and Safety Laboratory (HSL) for the European Union (EU) Fuel Cells and Hydrogen Joint Undertaking (FCH JU) project "HyIndoor" (http://www.hyindoor.eu) to investigate the behaviour of hydrogen jet fires within enclosures fitted with passive ventilation. The work was focussed on three areas of interest.

i) Flame length, temperature, radiation effects, oxygen depletion and hydrogen accumulation from well-ventilated jet-fires within enclosures.
ii) Heat balance considerations for well-ventilated jet-fires (for example, heat loss through hot gas flows and heat loss from enclosure walls by radiation / convection).
iii) Conditions required for jet-fires to become under-ventilated.

3.0 EXPERIMENTS AT HSL

3.1 Experimental Arrangement

A carbon steel enclosure with an internal volume of approximately 31 m^3 (2.5 m by 2.5 m by 5 m) was used. The enclosure was situated in the open air and so exposed to the weather during the experiments. Five passive vents (each 0.83 m wide and 0.27 m high) were located on the side walls. The vents could be fully or partially closed using steel plates and gaskets, or left open to the atmosphere. The walls are made from 6 mm thick steel plates and appear flat when viewed from inside, while the exterior features a number of more substantial horizontal and vertical structural beams. Two emergency explosion relief vents (total area 1.6 m^2) made from 100 μm aluminium foil were fitted in the roof. The enclosure is raised off the ground by 0.8 m. A schematic and a photograph of the enclosure are shown in Figure 1.

Hydrogen was released vertically upwards 0.5 m above, and in the centre of, the enclosure floor. Sub-sonic releases were through a 10 mm pipe using mass flow controllers and chocked flow releases were at pressures greater than 1 MPa through nozzles of less than 1 mm diameter. A propane pilot light was used to ignite the hydrogen and then turned off (typically within 2 seconds of hydrogen ignition).

The resulting hydrogen jet fire was then allowed to burn until the internal gas temperatures were at quasi-steady-state, or until the hydrogen within the enclosure reached a concentration considered to be potentially damaging to the facility should there be an explosion.
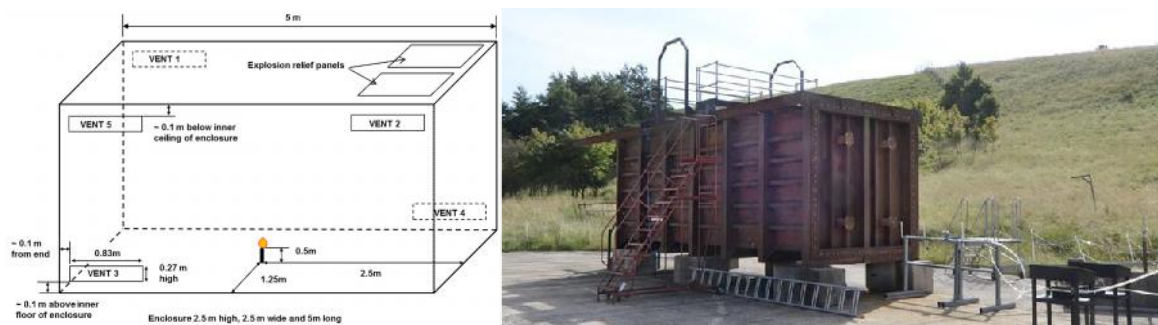

Figure 1. The HSL 31 m^3 enclosure

Oxygen and hydrogen concentrations were measured by extracting gas samples from five positions within the enclosure. The extracted gas was cooled and the water vapour removed before being passed through electrochemical oxygen analysers (with an accuracy of +/-0.1% v/v) and thermal conductivity hydrogen analysers (with a an accuracy of +/-1% v/v). Three sampling positions were at a height of 2.3 m from the floor, one was at 1.8 m and one at 1.0 m. Temperature measurements were made within the enclosure, using K-type thermocouples, at heights of 0.2 m, 1.0 m, 1.75 m and 2.3 m. A thermocouple was also placed in each open vent. Three humidity sensors were built into the enclosure walls, two at 1.3 m from the floor and one at 0.72 m. Three fast response ellipsoidal radiometers were placed within the enclosure, one close to the floor facing vertically upwards, and two facing horizontally across the enclosure. The positioning of the measurement positions are shown in Figure 2.
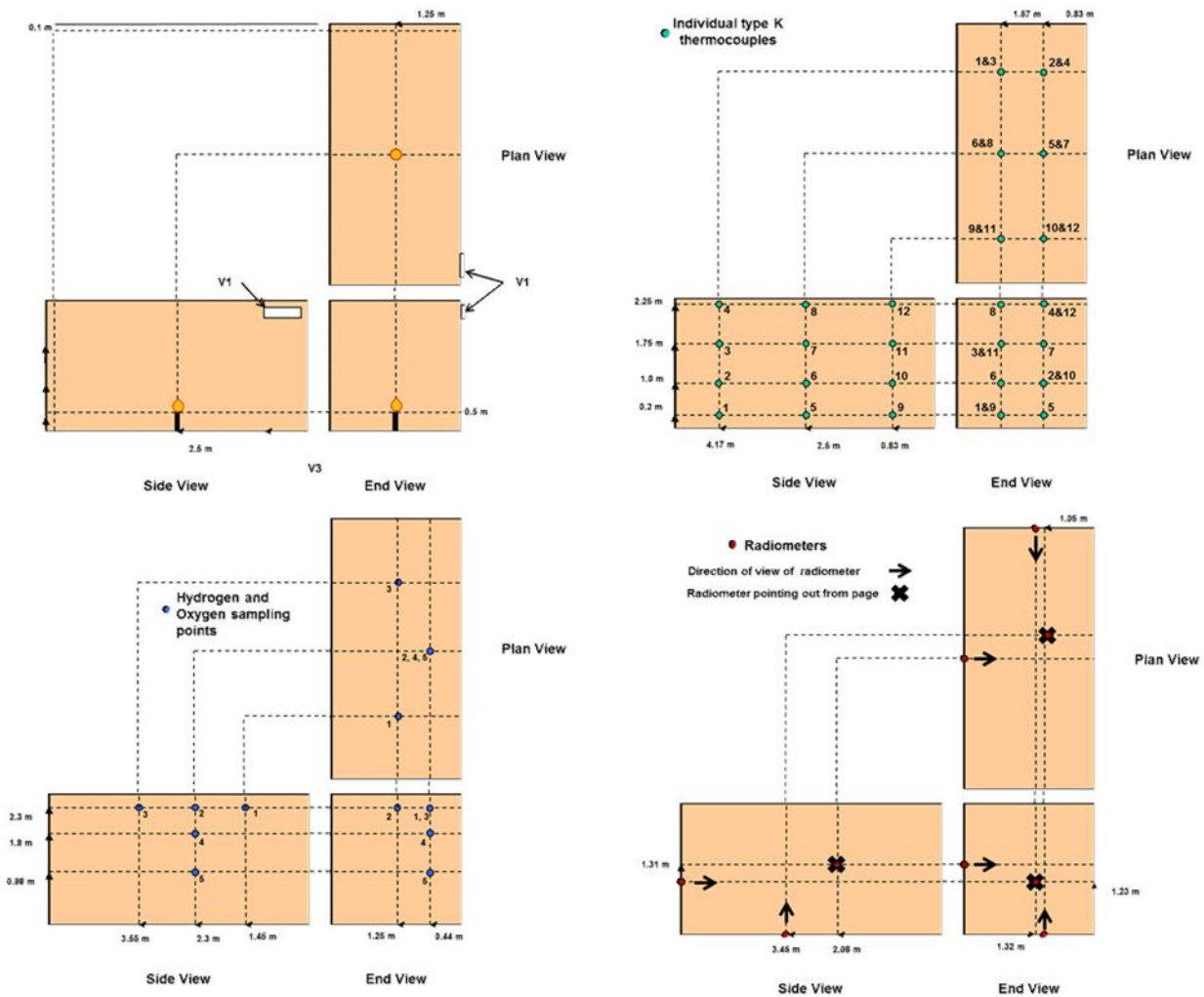
Figure 2. Positions of thermocouples, gas sampling points and radiometers relative to hydrogen flame and passive vent number 1

General atmospheric conditions were measured using a weather station located approximately 19m from the enclosure at a height of 3 m. A further ultrasonic wind direction sensor was located 5.5 m from the end of the enclosure at a height of 4.1 m.

Video footage of flames was captured using three visible range cameras located within the enclosure and a further visible range camera was used to monitor the upper open vent for external flames.

3.2 Results from Experiments

Twelve experiments were carried out, eight well-ventilated and four under-ventilated. The results are summarised in Table 1. The hydrogen flames were surprisingly visible; this is thought to be due to traces of dust in the enclosure and/or soot generated by the propane pilot flame.

A number of differences were observed in the well-ventilated tests involving chocked release jet-fires and sub-sonic jet-fires with similar flow-rates; the flame lengths for the chocked releases were shorter than those of the equivalent sub-sonic releases and it also appears that the layer of hot gas at the top of the enclosure was thinner for the sub-sonic releases than for the chocked releases. There was no evidence of hydrogen accumulation in any of the well-ventilated tests although there was a small degree of oxygen depletion. It is worth noting that release and ventilation conditions that resulted in flammable concentrations of accumulated hydrogen in un-ignited tests [3] did not result in under-ventilated fires in the tests reported here. It would appear that the opposite would also be true, i.e. designing a passive vent system to avoid flammable hydrogen accumulations would also avoid under-ventilated jet fires.

Significant oxygen depletion was evident in all of the under-ventilated tests and hydrogen accumulation was also observed. In test WP4/10, which had only one quarter of a vent open, severe oxygen depletion was followed by rapid hydrogen accumulation. The initial oxygen depletion resulted in a reduction in radiated heat, while later on, the onset of hydrogen accumulation was accompanied by a further reduction in radiated heat, a decrease in enclosure temperature and a stabilisation of the oxygen concentration. Those trends are shown in Figure 3. Note that the hydrogen release and fire was not started at time zero, but at approximately 300 seconds. The flame had reduced in size throughout the test, as shown in *Figure 4*, although it was still burning when the hydrogen supply was intentionally stopped. There was no visual evidence of flames external to the open upper vent in any of the tests.
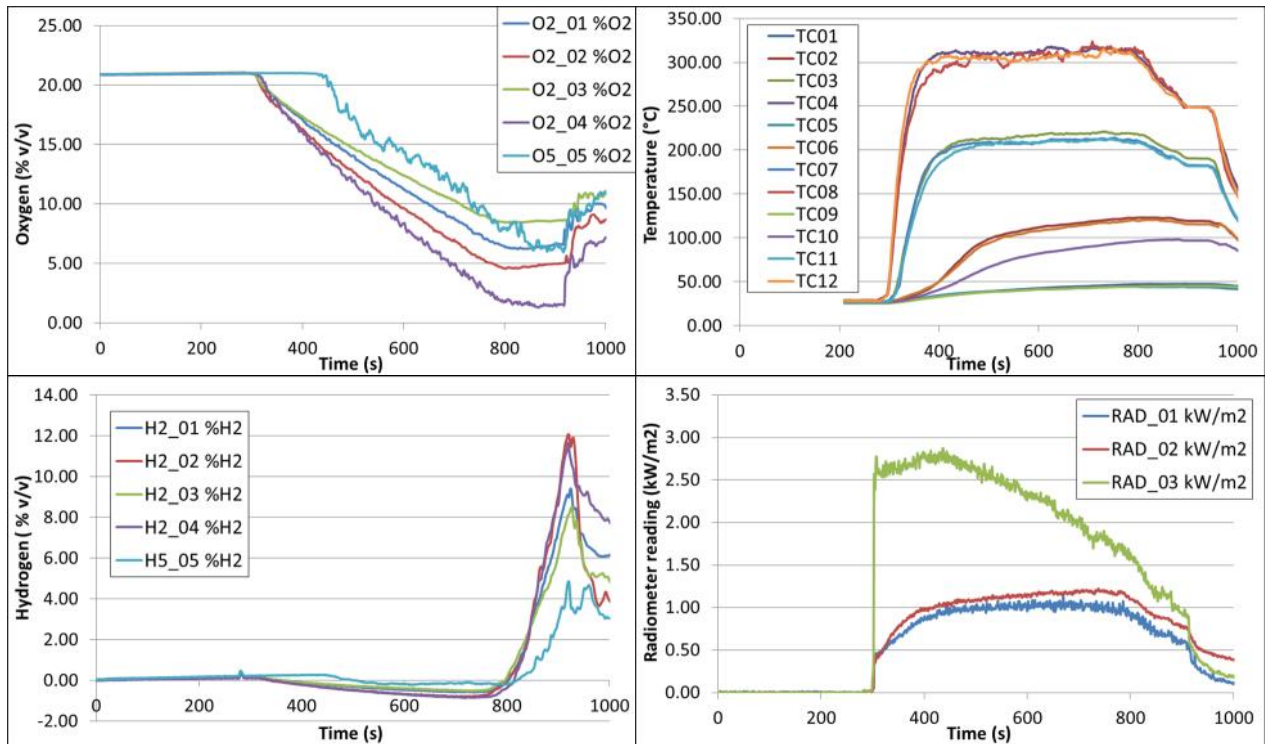

Figure 3. Oxygen, hydrogen, temperature and radiometer measurements from test WP4/10.

Figure 4. Flame shape, oxygen and hydrogen concentration at three times during test WP4/10.

4.0 COMPARISON WITH ANALYTICAL MODEL FOR ENCLOSURE TEMPERATURES

4.1 Analytical Modelling Approach

Analytical modelling of HSL's jet fire experiments was carried out using the model of Linden *et al.* [1], hereafter referred to as the Linden model. The Linden model can be used to predict the natural ventilation of an enclosure containing a buoyant source with one or more vents, including wall and ceiling vents. It makes a number of assumptions but has been validated against experiments involving the release of non-reacting buoyant gases, such as Cariteau and Tkatschenko [2] and Hooker *et al* [3]. One assumption made by the Linden model is that the ventilation is driven by the buoyant source and that the volume production associated with the buoyant source can be neglected. The Linden model separates buoyancy-driven ventilation into displacement and mixing regimes. In mixing ventilation the incoming air fully mixes with the fluid in the enclosure leading to a homogeneous environment whilst displacement ventilation is characterised by a stratified environment in which the incoming air only partially mixes with the fluid in the enclosure.

For mixing ventilation the Linden model predicts a steady-state reduced gravity inside the enclosure of,

$$g'_e = \left(\frac{B_0}{kAd^{1/2}} \right)^{2/3} \tag{1}$$

where B_0 is the buoyancy flux from the buoyant source, k is a vent exchange flow coefficient, A is the area of the vent and d is the height of the vent. For displacement ventilation the Linden model predicts a steady-state reduced gravity in the buoyant layer inside the enclosure of,

$$g'_e = \frac{B_0^{2/3}}{Ch^{5/3}} \tag{2}$$

where C is an entrainment constant associated with the buoyant source and h is the height of the interface between buoyant and ambient fluids.

For ignited releases the source of buoyancy driving the ventilation is temperature and the buoyancy flux can be described using,

$$B_0 = \frac{gQ_c}{T_a \rho_a c_{pa}} , \tag{3}$$

where g is gravitational acceleration, Q_c is the 'convective' power of the fire and T_a, ρ_a and c_{pa} are the ambient temperature, density and specific heat capacity, respectively. The 'convective' power of the fire was taken to be 70% of the total power, which is analogous to previous studies that have applied the Linden models to the ventilation of fires [4]. For tests with a single high vent the mixing ventilation model was used with an exchange flow coefficient of $k = 0.25$ [5], while for tests with high and low vents the displacement ventilation model was used with a vent discharge coefficient of $C_d = 0.6$.

Once the reduced gravity inside the enclosure has been calculated, the temperature inside the enclosure can be estimated using,

$$T_e = \frac{P_a M_e}{R \rho_a \left(1 - \dfrac{g'_e}{g} \right)} , \tag{4}$$

Where P_a and ρ_a are the ambient pressure and density, R is the universal gas constant and M_e is the molecular weight of the gas inside the enclosure. For the calculations carried out here, it was assumed that M_e was equal to the molecular weight of air.

Once the flow through the enclosure, due to passive ventilation, has been calculated, the steady-state average oxygen concentration in the enclosure can be estimated by subtracting the oxygen consumed by the burning hydrogen from that being introduced with the fresh air being drawn in.

Table 1. Summary of experimental results.

Test No.	Objective	Release type	Flow Rate (Nl/min)	Approximate Flame Length (m)	Orifice size (mm)	Release pressure (bar a)	Test duration* (s)	Passive Vent Configurations	Wind direction	Maximum Temperature (ºC)				Minimum Oxygen Concentration (% v/v)	Maximum Hydrogen Concentration (% v/v)	Comments
										0.2m from floor	1m from floor	1.75m from floor	2.25m from floor			
WP4/1	Investigate flame length / radiated heat etc for well-ventilated jet fire	Chocked	149	-	0.55	15	-	1 upper vent, V1 (0.87m x 0.23m)	-	-	-	-	-	-	-	Flame self-extinguished when pilot flame removed
WP4/2	Investigate flame length / radiated heat etc for well-ventilated jet fire	Subsonic	150	<~1m	10	1	1520	1 upper vent, V1 (0.87m x 0.23m)	From opposite side to open vent	~23	~40	~60	~100	19.4	0	
WP4/3	Investigate flame length / radiated heat etc for well-ventilated jet fire	Chocked	293	-	0.9	11	-	1 upper vent V5, 1 lower vent V4 (each 0.87m x 0.23m)	-	-	-	-	-	-	-	Flame self-extinguished when pilot flame removed
WP4/4	Investigate flame length / radiated heat etc for well-ventilated jet fire	Chocked	581	<0.5m	0.9	21.7	1344	1 upper vent V5, 1 lower vent V4 (each 0.87m x 0.23m)	81º to normal of upper open vent	<20	~20	~135	~150	19.6	0	
WP4/5	Investigate flame length / radiated heat etc for well-ventilated jet fire	Chocked	891	~1m	0.9	33.7	494 (continuous)	1 upper vent V5, 1 lower vent V4 (each 0.87m x 0.23m)	81º to normal of upper open vent	<20	~25	~180	~195	19.0	0	Issues with valve
WP4/6	Investigate flame length / radiated heat etc for well-ventilated jet fire	Chocked	648	~0.5m	0.9	24.4	1168 (continuous)	1 upper vent V1, 1 lower vent V3 (each 0.87m x 0.23m)	86º to normal of lower open vent	~38	~100	~165	~205	18.5	<1	Issues with valve
WP4/7	Investigate flame length / radiated heat etc for well-ventilated jet fire	Subsonic	648	~ 1.5m	10	1	1233	2 upper vent V1, 1 lower vent V3 (each 0.87m x 0.23m)	82º to normal of upper open vent	<25	25	~115	~230	18.8	0.3	
WP4/8	Investigate flame length / radiated heat etc for well-ventilated jet fire	Subsonic	891	~ 2m	10	1	928	3 upper vent V1, 1 lower vent V3 (each 0.87m x 0.23m)	84º to normal of upper open vent	<30	38	~140	~285	18.3	<1%	
WP4/9	Investigate flame length / radiated heat etc for under-ventilated jet fire	Subsonic	800	~ 2m	10	1	222 (continuous)	50% upper vent V1 only (0.42m x 0.27m)	Almost parallel to open vent	34	83	~213	~310	10.8	1.8	Issues with valve, run aborted
WP4/10	Investigate flame length / radiated heat etc for under-ventilated jet fire	Subsonic	800	~ 2m	10	1	612	25% upper vent V1 only (0.21m x 0.27m)	Almost parallel to open vent	~45	~120	~220	~320	1.4	12	
WP4/11	Investigate flame length / radiated heat etc for under-ventilated jet fire	Subsonic	800	~ 2m	10	1	1400	50% upper vent V1 only (0.42m x 0.27m)	Almost parallel to open vent	~50	~130	~210	~325	7.3	14	
WP4/12	Investigate flame length / radiated heat etc for under-ventilated jet fire	Subsonic	800	~ 2m	10	1	761	25% upper vent V1 only (0.21m x 0.27m)	Almost parallel to open vent	~40	~115	~215	~325	7.9	16.1	

* Where there were problems with the valve, the test duration refers to the longest continuous hydrogen release.

4.2 Analytical Modelling: Results and Discussion

An overview of the analytical model calculations and results is shown in *Table 2*. The fire power was calculated using the lower heating value for hydrogen, namely 120 MJ/kg [6]. The mixing ventilation model used for tests with a single high vent assumes full mixing and the temperature is the predicted value throughout the enclosure. Conversely, the displacement ventilation model used for tests with high and low vents assumes a stratified environment. For these tests *Table 2* shows the height of the interface between buoyant and ambient fluids and the temperature in the buoyant layer.

 The results in *Table 2* show that the Linden model predicts significantly higher ventilation rates, expressed in "air changes per hour" (ACH), and therefore lower temperatures for a given fire power, for tests with high and low vents than for tests with a single high vent. This is consistent with observations made previously that multi-vent configurations lead to much more efficient ventilation than single vent configurations [3]. Furthermore, this simple model neglects heat transfer via the enclosure walls. For these reasons, the Linden model can be expected to over-predict the temperature. The measured "steady-state" oxygen concentrations are compared, in *Table 2*, with the concentrations estimated by balancing the predicted rate of oxygen consumption in the fire and the oxygen introduction via the passive ventilation. For well-ventilated jet-fires the estimates are in broad agreement with the measured minimum values. The estimated values for the under-ventilated fires are not so good, but still show a significant degree of under-ventilation occurring.

Table 2. Overview of calculations and results.

Test	Open vents	Hydrogen release rate (Nl/min)	Total power of fire (kW)	Predicted steady-state interface height (m)	Predicted steady-state temperature (C)	Predicted steady-state ventilation rate (ACH)	Estimated average "steady-state" oxygen concentration (% v/v)	Range of measured "steady-state" oxygen concentrations for all sample points (% v/v)	Comments
WP4/2	V1	150	26	n/a	204	9	19.4	19.4 – 20.2	
WP4/4	V4, V5	581	101	1.6	189	37	19.5	19.6 – 20.8	
WP4/5	V4, V5	891	155	1.6	248	42	18.9	19.0 – 20.8	
WP4/6	V1, V3	648	112	1.6	202	38	19.3	18.5 – 20.8	
WP4/7	V1, V3	648	112	1.6	202	38	19.3	18.8 – 20.8	
WP4/8	V1, V3	891	155	1.6	248	42	18.9	18.3 – 20.8	
WP4/9	50% V1	800	139	n/a	942	10	13.3	10.8 – 18.4	Steady-state not reached
WP4/10	25% V1	800	139	n/a	1489	6	8.1	1.4 - 7.8	
WP4/11	50% V1	800	139	n/a	942	10	13.3	7.3 - 11.8	
WP4/12	25% V1	800	139	n/a	1489	6	8.1	7.9 - 14.8	Possible leakage via damaged explosion relief panel

Figure 5 shows a comparison between maximum temperature measurements from HSL's experiments and the Linden model predictions. Most of the measurements from well ventilated fires are predicted to within a factor of two. Temperature measurements from under-ventilated fires were over-predicted probably due to both the increased influence of heat losses through the enclosure walls and the incomplete combustion of the hydrogen which aren't accounted for in the model.

4.3 Conclusions from the Analytical Modelling

The Linden model has been used to carry out post-test modelling of HSL's jet fire experiments, to calculate the steady-state ventilation rate, temperature and average oxygen concentration inside the enclosure. Temperature predictions and oxygen concentrations were in reasonable agreement with the measurements for well-ventilated fires. For under-ventilated fires the temperature predictions were poor although the oxygen concentration estimates did indicate significant degrees of under-ventilation and could potentially be used to identify under-ventilation problems for design purposes.
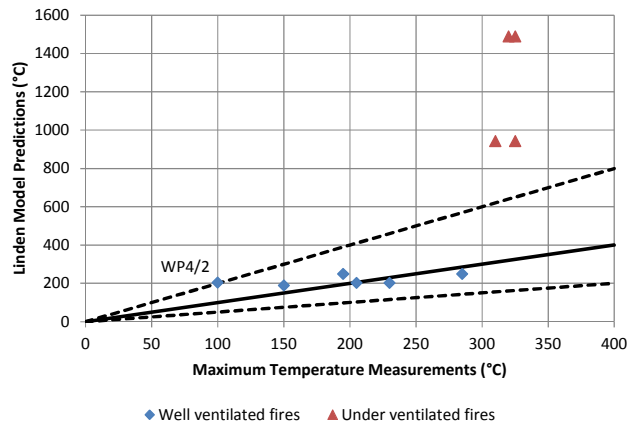

Figure 5. Comparison of maximum temperature measurements and Linden model predictions. Solid line indicates exact agreement between predictions and measurements, dashed lines indicate a factor of two difference.

5.0 CFD INVESTIGATION OF INFLUENCE OF THERMAL PROPERTIES OF THE ENCLOSURE

CFD modelling was carried out to investigate the thermal properties of the enclosure on the behaviour of the jet fires. Simulations were carried out of experiment WP4/2 which was performed using a single high vent (V1), a hydrogen release rate of 150 NL/min and a nozzle diameter of 10 mm. This experiment has various features that make it amenable to CFD modelling, including a single vent (thereby minimising the impact of the uncertainty introduced by varying wind conditions) and a low momentum source with well-ventilated conditions (allowing a relatively simple, less computationally expensive combustion model to be used).

5.1 CFD Modelling Approach

CFD modelling was carried out using the general purpose CFD code ANSYS CFX 15 [7]. All of the simulations were performed using hybrid meshes with structured prism elements inside the enclosure and unstructured tetrahedral elements outside. Mesh refinement is specified on the nozzle, along the path of the jet, near the vents and on the external walls of the enclosure. Two meshes were used for the simulations, namely 'medium' and 'fine' resolution meshes having approximately 430,000 and 620,000 elements respectively.

The dispersion of hydrogen and subsequent combustion products was modelled using a multicomponent flow approach, which assumes that hydrogen, oxygen, nitrogen and water vapour mix at the molecular level and they share the same mean velocity, pressure and temperature fields [7]. Turbulence was modelled using the k-ε model with buoyancy production and dissipation, whilst heat transfer was modelled using the Total Energy model [7]. The turbulence intensity at the jet source was set to 10%. The release pipe, the enclosure walls and the ground were modelled using a no slip, hydraulically smooth boundary condition.

The eddy dissipation model was used to model the combustion of hydrogen. Despite its simplicity it performs well for modelling turbulent reacting flows including premixed combustion and diffusion flames and is widely used in industry.

It is important to consider the radiation properties of the materials present. Homo-nuclear diatomic molecules such H_2, O_2 and N_2 are unable to interact in the thermal region of the spectrum. However, the effect of radiation on hetero-nuclear molecules, such as H_2O, needs to be incorporated into the model. For the purposes of minimising computational expense, the so-called grey approximation was used, that is the gas is assumed to have the same properties throughout the spectrum. The media is assumed to be isotropic and homogeneous so the concentration dependence can also be ignored and the Beer-Lambert law used to model radiation transport.

Four types of thermal boundary are possible in ANSYS CFX: adiabatic; prescribed temperature; prescribed heat flux and prescribed heat transfer coefficient. The use of adiabatic boundaries was investigated (simulation S5), however, the results were found to give very high temperatures not reflected in the experimental results. For simplicity, a prescribed temperature approach was adopted.

Although, in reality, walls can absorb, reflect and emit thermal radiation, in this work the walls are modelled as being a black body radiator at ambient temperature. This means the walls absorb all the radiation directed at them (i.e. they do not reflect any radiation) and they emit radiation at a rate proportional to their prescribed temperature, 283K. A more complete treatment would add considerable complexity and computational expense to the simulations.

The simulations were carried out using 'high resolution' discretisation in space and second order discretisation in time [7]. Convergence was judged by monitoring normalised Root Mean Square (RMS) residual values. ANSYS recommend that convergence requires RMS values of 10^{-4} or less and this was the criterion adopted here. Steady state simulations were performed with a maximum 'time-step' of 0.05 s, whilst transient simulations were carried out using time-steps of 0.02 s.

5.2 CFD Modelling Results

The CFD modelling approach assumes that the conditions within the enclosure are not sensitive to variations in the wind speed or the approach used to account for radiation. The validity of these assumptions is assessed by using steady state simulations to assess the sensitivity of the results to changes in the wind speed (0.5 to 2.0 m/s), the absorption coefficient (0.5 to 1.0), grid resolution and interior thermal boundary condition (fixed at 283K and adiabatic). The range of predicted temperatures at each height, for various model conditions, is shown in Table 3. Also shown in Table 3 is the predicted ventilation rate of the enclosure.

Table 3 Overview of simulation results

Simulation	Grid resolution	Wind-speed (ms^{-1})	Enclosure interior thermal boundary condition	H_2O Absorption coefficient (m^{-1})	Temperature (K)				Ventilation rate (ACH)
					High 2.3(m)	Medium 1.75(m)	Low 1.0(m)	Lowest 0.2(m)	
S1	High	0.5	283K (fixed)	1.0	[335,358]	[325,330]	[308,313]	[295,305]	10
S2	Medium	0.5	283K (fixed)	1.0	[340,355]	[325,330]	[308,313]	[295,305]	9.5
S3	Medium	0.5	283K (fixed)	0.5	[342,358]	[322,330]	[308,313]	[295,305]	9.5
S4	Medium	2.0	283K (fixed)	0.5	[345,355]	[325,332]	[311,314]	[297,303]	9
S5	Medium	0.5	Adiabatic	1.0	S2+300K				30+

Simulations carried out with different mesh resolutions gave very similar predictions and indicate that the solution is not mesh dependent. Changing the wind speed also has only a slight effect on the internal temperature. The single biggest identified factor affecting the internal temperatures is the thermal boundary condition on the inside of the enclosure. The two cases considered, adiabatic and fixed temperature (simulations S5 and S2 respectively), represent bounding cases. The simulation S5, with adiabatic walls, produced temperatures which were vastly (300K) in excess of simulations with fixed wall temperature (for example S1-S4). The adiabatic case effectively provides a model of an insulated room where the temperatures within the room are, for a given fire power, determined solely by the ventilation rate. The constant temperature boundary condition case however would be expected to over-predict the heat losses within the enclosure as the walls effectively act as if they were refrigerated such that the temperature remains constant. In this case, the internal temperature is dependent on not only the ventilation rate, but also the heat lost to the walls.

A transient simulation was carried out, based on the same approach as that used in steady state simulation S2. This method of simulation was carried out since this was most likely to give the best fit with the experimentally measured temperatures, based on the sensitivity studies. Due to the long computing time required only the first 400 seconds of the release were modelled. This was in part due to the adaptive time-stepping method used to ensure that all of the residuals were well controlled and the simulations had achieved an acceptable level of convergence.

Figure 6 shows model predictions of temperatures and velocities on a plane through the enclosure and the centre of the vent. The strong thermal stratification is clearly evident, particularly in the main body of the room where the buoyant warm air has risen and collected below the ceiling of the enclosure. The rate at which this warm air can exit the enclosure is determined by how rapidly fresh air can be introduced into the room. That is, hot air rises out of the container as cooler outside air is drawn in to maintain the internal pressure. Calculations from the simulation indicate that a steady state of around 9 ACH is quickly reached (within 150 s) and maintained throughout the steady part of the calculation. This figure of 9 ACH is in good agreement with the value found using the analytical model reported in Section 4.2. The velocity vectors in *Figure 6* show the cascade of cold air falling in through the opening.

In order to quantify the thermal stratification, it is useful to compare the steady state and transient model predictions to the experimental measurements as shown in *Figure 7*. The results of the steady state simulation are shown as bands that indicate the range of CFD results at different heights in the enclosure and the transient CFD model predictions are shown as coloured lines.

The transient simulation reaches a steady state at around 100 - 200 s that is comparable to the steady state simulations. The thermal stratification predicted by the simulations is qualitatively similar to that shown by the experimental measurements. The initial temperature rises for the higher sensors show good agreement between the model predictions and experiments. However, for the lower levels, the rise in temperature predicted by the CFD model is considerably faster than observed. It is not clear whether the experiment reached a steady state, as the lowest temperature sensors appear to be still rising at the end of the experiment. The good agreement between the model and experiment could be due to the combustion model over predicting flame temperatures and the thermal boundary condition extracting too much energy. There is also the possibility that the thermal boundary condition is artificially increasing the level of turbulence and leading to a state that has a higher degree of mixing than was present within the experiment. The result of this is that the simulation reached a steady state far faster than the experiment. As such, the good agreement observed here between the experiment and CFD must be treated as an early result until more work can verify the approach.
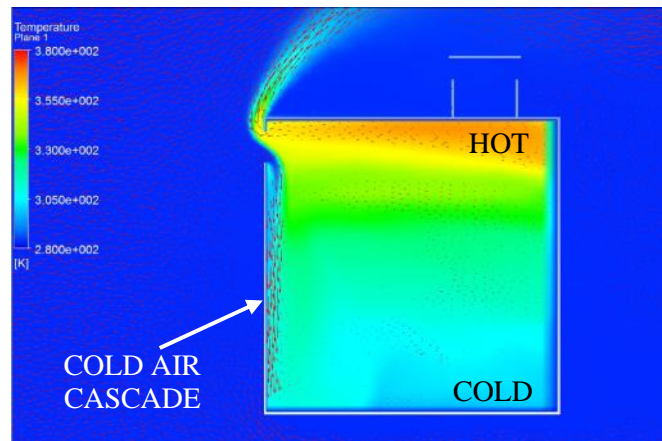
Figure 6 CFD model predictions of temperatures and velocities for experiment WP4-2 on a cross section through the enclosure.
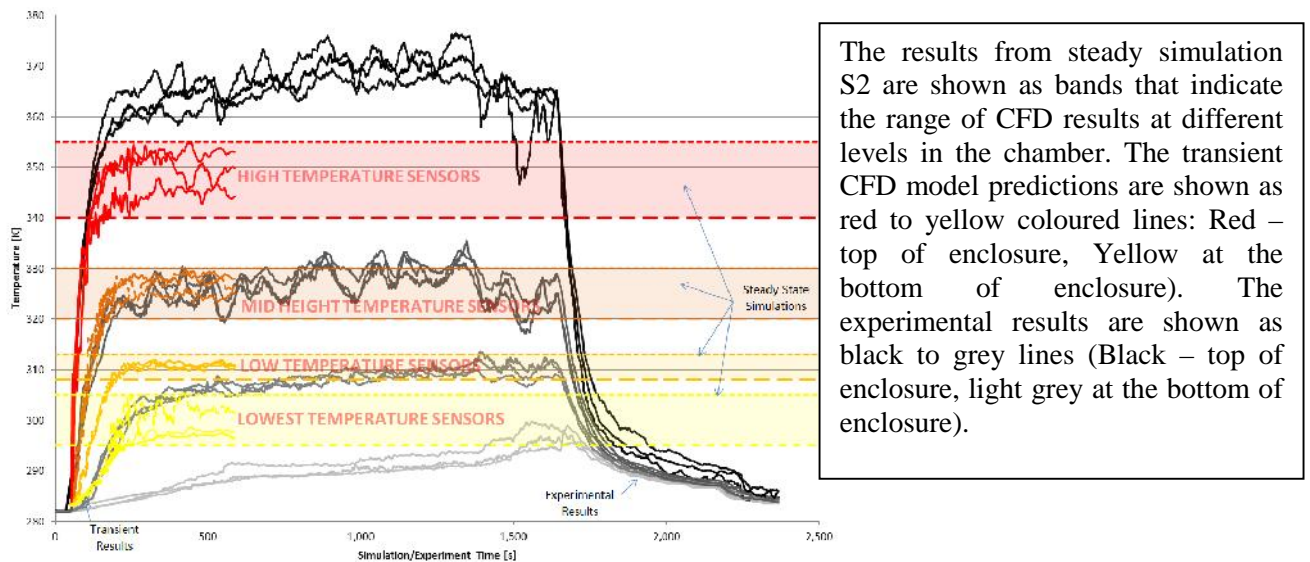

The results from steady simulation S2 are shown as bands that indicate the range of CFD results at different levels in the chamber. The transient CFD model predictions are shown as red to yellow coloured lines: Red – top of enclosure, Yellow at the bottom of enclosure). The experimental results are shown as black to grey lines (Black – top of enclosure, light grey at the bottom of enclosure).

Figure 7 Comparison of CFD model temperature predictions and experimental measurements for experiment WP4-2.

5.7 Conclusions from CFD studies

The key conclusion from this work is that the treatment of the thermal boundary condition on the enclosure walls has a significant effect on the results. This is important because in practical applications the properties of the walls may vary considerably. Iso-container type enclosures are likely to have relatively thin walls made from materials with a high thermal conductivity (e.g. steel) and setting the wall temperature equal to the ambient temperature can provide reasonable results (although internal temperatures can be under-predicted). Alternatively, it is possible to model conjugate heat transfer into/through the wall taking into account the thickness of the wall, its thermal conductivity and transient effects. However, this approach is significantly more complicated. Other facilities may have thicker walls made from materials with far lower thermal conductivities (e.g. concrete or brick). The heat flux into/through such walls may be significantly lower and may lead to much higher internal temperatures. For these types of enclosure simulations can be carried out using an adiabatic boundary condition (although internal temperatures would probably be over-predicted) or the conjugate heat transfer approach taking into account the properties of the wall and any transient effects.

6.0 OVERALL CONCLUSIONS

A series of experiments have been carried out to investigate indoor hydrogen jet fires. These have provided data for well-ventilated and under-ventilated jet fires and have also shown differences in behaviour between sub-sonic and chocked flow releases.

It appears that designing a passive vent system to avoid flammable hydrogen accumulations would also avoid under-ventilated jet fires.

Analytical modelling, based on the approach of Linden *et al* [1] has been used to calculate temperatures and oxygen concentrations within the enclosure. Despite the simple assumptions in the model, the results are reasonable for well-ventilated fires. The models are poor at estimating temperatures for under-ventilated fires, although the calculation of oxygen concentration does indicate significant under-ventilation and may be useful in identifying such problems with enclosure designs.

CFD modelling has been used to investigate the thermal properties of the enclosure on the behaviour of the jet fires. It was concluded that modelling the thermal boundary condition on the enclosure walls is critical to getting reasonable results, a finding that is highly significant to practical hydrogen systems within enclosures/rooms.

7.0 ACKNOWLEDGEMENTS

8.0 REFERENCES

1. Linden, P.F., Lane-Serff, G.F. and Smeed, D.A., Emptying filling boxes: the fluid mechanics of natural ventilation. *J. Fluid Mech.*, 212, 1990, 309-335.
2. Cariteau, B. and Tkatschenko I., Experimental study of the effects of vent geometry on the dispersion of a buoyant gas in a small enclosure. *International Conference on Hydrogen Safety*, San Francisco. September, 2011.
3. Hooker, P., Hoyes, J.R. and Hall, J., Accumulation of hydrogen released into an enclosure fitted with passive vents – experimental results and simple models. *IChemE Hazards XXIV*, 17-19 May, 2014, Edinburgh, UK.
4. Rooney, G.G. and Linden, P.F., Strongly buoyant plume similarity and 'small-fire' ventilation. *Fire Saf. J.* 29 1997, 235–58.
5. Dalziel, S.B. and Lane-Serff, G.F., The Hydraulics of Doorway Exchange Flows. *Building and Environment*, 26, 1991, 121-135.
6. Heywood, J.B. (1988). Internal Combustion Engine Fundamentals. McGraw-Hill Book Company, Singapore.
7. ANSYS (2013). ANSYS CFX-Solver Theory Guide. ANSYS, Inc., Canonsburg, Pennsylvania, USA. Release 15.0, November 2013.